

Preparation and thermoelectric properties of $\beta\text{-Fe}_{1-x}\text{Ru}_x\text{Si}_2$

H. TAKIZAWA, P. F. MO, T. ENDO, M. SHIMADA

Department of Molecular Chemistry and Engineering, Faculty of Engineering, Tohoku University, Sendai, Miyagi 980, Japan

$\beta\text{-Fe}_{1-x}\text{Ru}_x\text{Si}_2$ solid solution was synthesized by solid state reaction at 1100 °C for 48 h and subsequent annealing at 850 °C for 168 h in an evacuated silica tube. Single phase solid solution was obtained in the composition range $0 \leq x \leq 0.1$. The thermal stability range of the β -phase is extended to higher temperature region by partial substitution of Ru atom. The thermoelectric properties of Cr or Co-doped $\beta\text{-Fe}_{1-x}\text{Ru}_x\text{Si}_2$ strongly depend on the sintering conditions. The samples with optimum thermoelectric properties are obtained by high-pressure sintering at 3 GPa and 800 °C for 1 h. The optimum compositions are found to be $\text{Fe}_{0.92}\text{Ru}_{0.05}\text{Cr}_{0.03}\text{Si}_2$ and $\text{Fe}_{0.92}\text{Ru}_{0.05}\text{Co}_{0.03}\text{Si}_2$ for *p*-type and *n*-type materials, respectively. The power factors ($\sigma\alpha^2$) of these materials are higher than that of $\beta\text{-FeSi}_2$ based materials.

1. Introduction

Semiconducting iron disilicide ($\beta\text{-FeSi}_2$) is one of the attractive materials for high temperature thermoelectric conversion because of its large thermoelectric power, relatively low electrical resistivity, and high oxidation resistance [1–2]. Both *p*-type and *n*-type $\beta\text{-FeSi}_2$ are available by partial substitution of transition metal elements. Usually chromium or manganese is used as *p*-type dopant and cobalt as *n*-type dopant.

Pure $\beta\text{-FeSi}_2$ is stable below 970 °C and peritectoidally decomposes into nonstoichiometric $\alpha\text{-Fe}_{1-x}\text{Si}_2$ and FeSi (ϵ -phase) above 970 °C [3]. $\alpha\text{-Fe}_{1-x}\text{Si}_2$ and FeSi exhibit metallic conduction. The figure of merit (*Z*) for thermoelectric conversion of both *p*-type and *n*-type $\beta\text{-FeSi}_2$ exhibits broad maxima at around 500 °C and drastically decreases after the decomposition. For high temperature applications, it is important to extend the thermal stability range of the β -phase to a higher temperature region.

$\beta\text{-FeSi}_2$ has the orthorhombic A11 unit cell (space group: Cmca), which is a distorted variant of the fluorite (CaF_2) type structure [4]. There are two different crystallographic iron sites in $\beta\text{-FeSi}_2$. OsSi_2 is isostructural with $\beta\text{-FeSi}_2$ [5]. These two materials are the only known compounds with the orthorhombic A11 crystal structure [6], and OsSi_2 , with orthorhombic $\beta\text{-FeSi}_2$ type structure, is stable up to the melting point ($T_m > 1700$ °C). It is expected that $\beta\text{-FeSi}_2$ is thermally stabilized by partial substitution of 8-group elements of Os and Ru for Fe atoms. However, Os-substitution is not suitable for high temperature applications, because osmium compounds are toxic at high-temperature oxidation atmospheres. Therefore, Ru is a candidate for a substituent element, although the existence of RuSi_2 is not reported in the binary Ru–Si system [7].

In the present study, partial substitution of the Ru atom in the system $\text{Fe}_{1-x}\text{Ru}_x\text{Si}_2$ was attempted to improve the thermal stability and thermoelectric properties of $\beta\text{-FeSi}_2$.

2. Experimental procedure

$\beta\text{-Fe}_{1-x}\text{Ru}_x\text{Si}_2$ solid solution was synthesized by solid state reaction under vacuum conditions. Iron (> 99.9% purity), ruthenium (99.9% purity), and silicon (> 99.99% purity) were used as starting materials. These powders were mixed in the desired molar ratio and pressed into pellet form at 100 MPa. The pellet was calcined at 1100 °C for 48 h, and then annealed at 850 °C for 168 h in an evacuated silica tube. The product thus obtained was pulverized and identified by X-ray powder diffraction analysis using Fe-filtered $\text{CoK}\alpha$ radiation.

To measure the thermoelectric properties the obtained solid solution was sintered under two different conditions: pressureless sintering at the same condition as the sample preparation and high-pressure sintering at 3 GPa and 800 °C for 1 h. The Belt-type high-pressure equipment was used for high-pressure sintering. The detailed cell assemblage of the Belt-type equipment has been described elsewhere [8].

The electrical conductivity and the thermoelectric power of the sintered specimens were measured by conventional d.c. methods in the temperature range 300–1100 K.

3. Results and discussion

3.1. Thermal stability of $\beta\text{-Fe}_{1-x}\text{Ru}_x\text{Si}_2$

The samples with chemical composition $\beta\text{-Fe}_{1-x}\text{Ru}_x\text{Si}_2$ ($0 \leq x \leq 0.2$), were reacted at 1100 °C for 48 h and subsequently annealed at 850 °C for 168 h

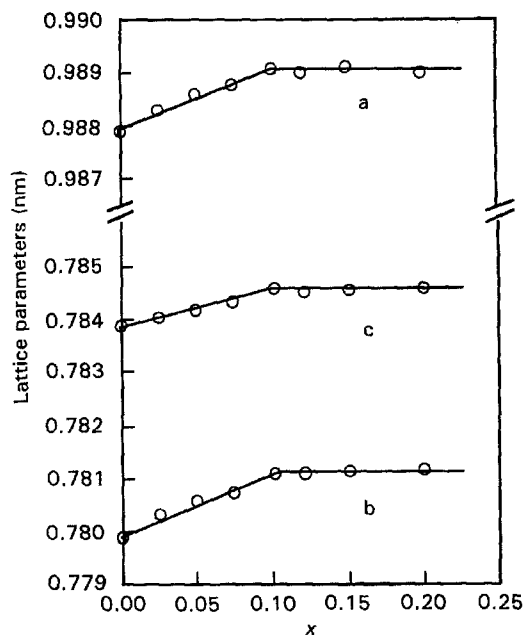


Figure 1 Compositional dependence of the lattice parameters in the system $\beta\text{-Fe}_{1-x}\text{Ru}_x\text{Si}_2$.

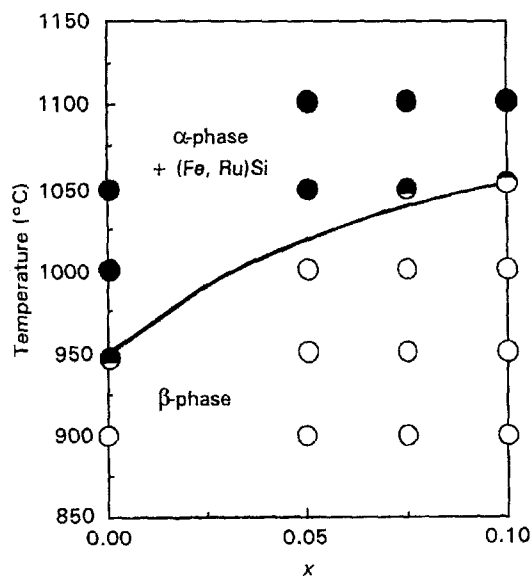


Figure 2 Thermal stability of $\beta\text{-Fe}_{1-x}\text{Ru}_x\text{Si}_2$.

in an evacuated silica tube. The products obtained by the reaction at 1100°C for 48 h were composed of $\alpha\text{-(Fe,Ru)}_{1-y}\text{Si}_2$ and $(\text{Fe,Ru})\text{Si}$ in the whole chemical composition range. Single phase $\beta\text{-Fe}_{1-x}\text{Ru}_x\text{Si}_2$ solid solution was obtained in the composition range $0 \leq x \leq 0.1$ after annealing at 850°C for 168 h. In the composition range $x > 0.1$, Ru_2Si_3 coexisted with $\beta\text{-Fe}_{1-x}\text{Ru}_x\text{Si}_2$ ($x = 0.1$) and Si. Fig. 1 shows the compositional dependence of the lattice parameters in the $\beta\text{-Fe}_{1-x}\text{Ru}_x\text{Si}_2$ solid solution system. The lattice parameters of orthorhombic $\beta\text{-Fe}_{1-x}\text{Ru}_x\text{Si}_2$ increase with increasing Ru content up to $x = 0.1$. In the composition range of $x > 0.1$, lattice parameters of the orthorhombic β -phase are constant. The solubility limit of Ru in the system $\text{Fe}_{1-x}\text{Ru}_x\text{Si}_2$ was determined to be $x = 0.1$. The variation of the lattice parameters obeys Vegard's law in the composition range of $0 \leq x \leq 0.1$,

indicating random displacement of Ru atoms on two different crystallographic iron sites.

To evaluate the thermal stability of the β -phase, $\beta\text{-Fe}_{1-x}\text{Ru}_x\text{Si}_2$ ($0 \leq x \leq 0.1$) solid solution was annealed at various temperatures between 900 and 1100°C for 168 h in an evacuated silica tube and quenched in water. The resulting product was analysed by X-ray powder diffraction analysis. Fig. 2 shows the thermal stability field of the β -phase in relation to the Ru content. The β -phase is stable below 950°C at $x = 0$ (FeSi_2). The stability range of the β -phase is successfully extended to higher temperature regions by increasing the Ru content: the β -phase is stable up to 1050°C at a composition of $x = 0.1$.

It is generally known that the valence electron concentration and the atomic radius ratio of the constituent elements are important factors in determining the structural stability of alloys and intermetallic compounds [9–10]. The present experimental results in the isoelectronic solid solution system suggest that the enhancement of atomic radius ratio, $r_{\text{Fe}}/r_{\text{Si}}$, is effective in stabilizing the orthorhombic $\beta\text{-FeSi}_2$ type structure at high temperature conditions.

3.2. Thermoelectric properties

$\beta\text{-Fe}_{1-x}\text{Ru}_x\text{Si}_2$ solid solutions doped with Cr (*p*-type) and Co (*n*-type) were sintered under two different conditions. Fig. 3 shows scanning electron micro-

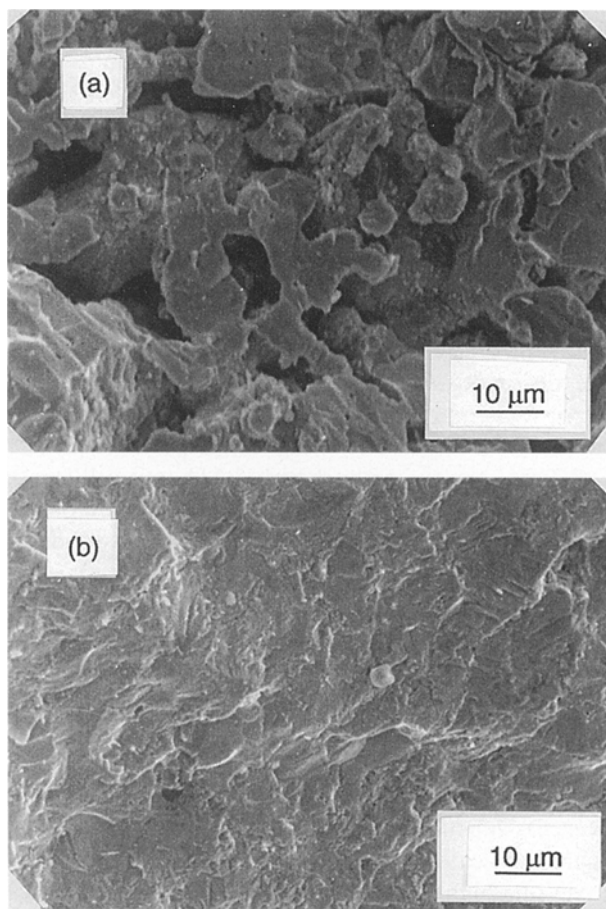


Figure 3 Microstructure of $\text{Fe}_{0.92}\text{Ru}_{0.05}\text{Cr}_{0.03}\text{Si}_2$ sintered under (a) pressureless and (b) high-pressure conditions.

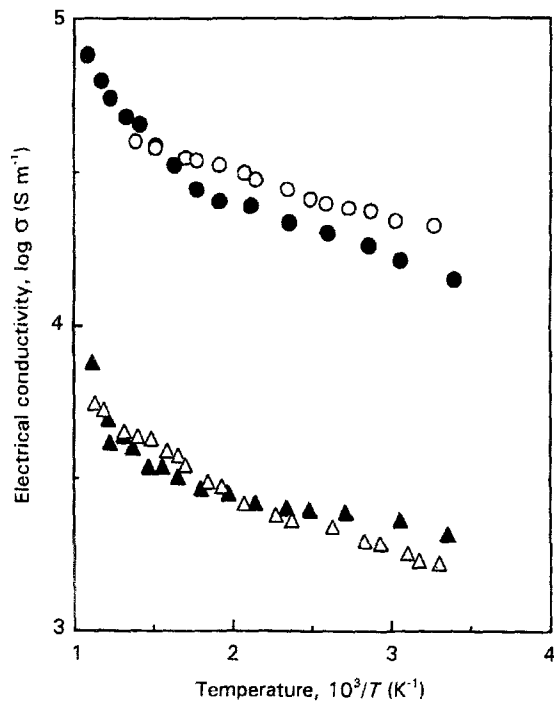


Figure 4 Temperature dependence of the electrical conductivity of Cr- or Co-doped $\beta\text{-Fe}_{1-x}\text{Ru}_x\text{Si}_2$ (H.P.: sintered under high-pressure condition. (○) H.P. Co 3% Ru 5%; (●) H.P. Cr 3% Ru 5%; (Δ) Co 3% Ru 5%; (▲) Cr 3% Ru 5%.

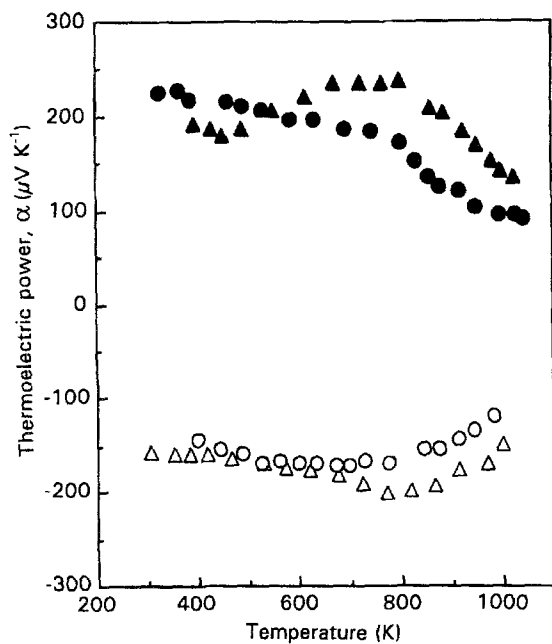


Figure 5 Temperature dependence of the thermoelectric power of Cr- and Co-doped $\beta\text{-Fe}_{1-x}\text{Ru}_x\text{Si}_2$ (H.P.: sintered under high-pressure conditions (●) H.P. Cr 3% Ru 5%; (▲) Cr 3% Ru 5%; (○) H.P. Co 3% Ru 5%; (Δ) Co 3% Ru 5%.

graphs of crushed surfaces of the representative specimens sintered under two different conditions. The specimens sintered under pressureless conditions show a porous microstructure with density 80% of the theoretical value, while the specimens sintered at 3 GPa and 800 °C are fully densified and their surfaces show metallic lustre.

The results of the measurements of the electrical conductivity (σ) and the thermoelectric power (α) for

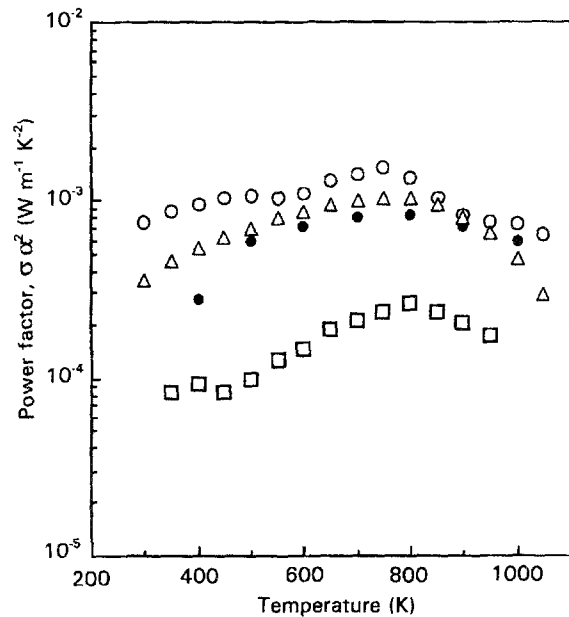


Figure 6 Power factor of Cr-doped $\beta\text{-Fe}_{1-x}\text{Ru}_x\text{Si}_2$ (*p*-type). (○) H.P. Cr 3% Ru 5%; (Δ) H.P. Cr 5% Ru 5%; (□) Cr 3% Ru 5%; (●) *p*-FeSi₂.

both *p*-type and *n*-type materials are shown in Figs 4 and 5. The notation H.P. means the specimens were sintered under high-pressure conditions (3 GPa and 800 °C). The electrical conductivity of the sintered specimens strongly depends on the sintering conditions. The conductivity of the specimens sintered at high-pressure conditions is higher than that of the specimens sintered at pressureless conditions by an order of magnitude. This result is due to the difference in bulk density of the sintered specimens.

The behaviour of the α -*T* curve depends on the sintering conditions, especially for *p*-type materials. The absolute values of α are low in the specimens sintered at high pressure conditions. This result is curious because such a difference in thermoelectric power is not attributed to the difference in bulk density of the sintered specimens, i.e., the thermoelectric power of materials is essentially independent of the effective cross-section. One of the possible reasons is due to the precipitation of small amounts of Si at the grain boundaries of the specimens sintered under pressureless conditions. In the case of pressureless sintering at 1100 °C for 48 h and annealing at 850 °C for 168 h, the following phase changes, $\alpha + (\text{Fe,Ru})\text{Si} \rightarrow \beta + (\text{Fe,Ru})\text{Si} + \text{Si} \rightarrow \beta$, occur during the sintering process. These phase changes may introduce the precipitation of a small amount of Si at the grain boundaries of β -phase grains and may enhance the thermoelectric power. On the other hand, phase change does not occur under high-pressure sintering conditions (3 GPa and 800 °C), which is in the stability range of the β -phase.

The thermoelectric properties of various specimens with different concentration of dopant are examined for both *p*-type and *n*-type materials. The power factors, $\sigma\alpha^2$, for thermoelectric conversion are calculated for some representative specimens. The results are shown in Figs 6 and 7 for *p*-type and *n*-type materials.

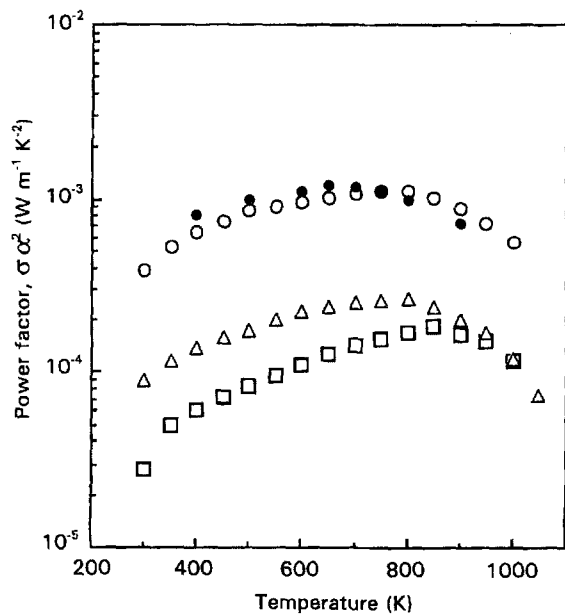


Figure 7 Power factor of Co-doped β -Fe $_{1-x}$ Ru $_x$ Si $_2$ (n-type). (○) H.P. Co 3% Ru 5%; (△) Co 5% Ru 5%; (□) Co 3% Ru 5%; (●) n-FeSi $_2$.

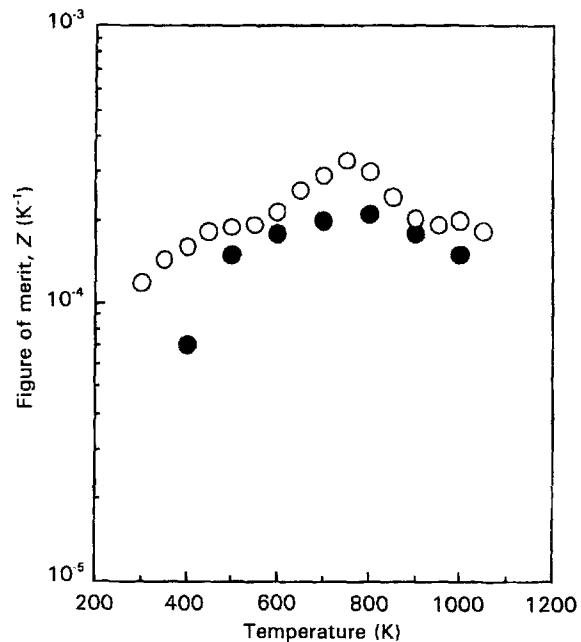


Figure 9 Figure of merit (Z) for thermoelectric conversion of p-type Fe $_{0.92}$ Ru $_{0.05}$ Cr $_{0.03}$ Si $_2$. (○) H.P. Cr 3% Ru 5%; (●) p-FeSi $_2$.

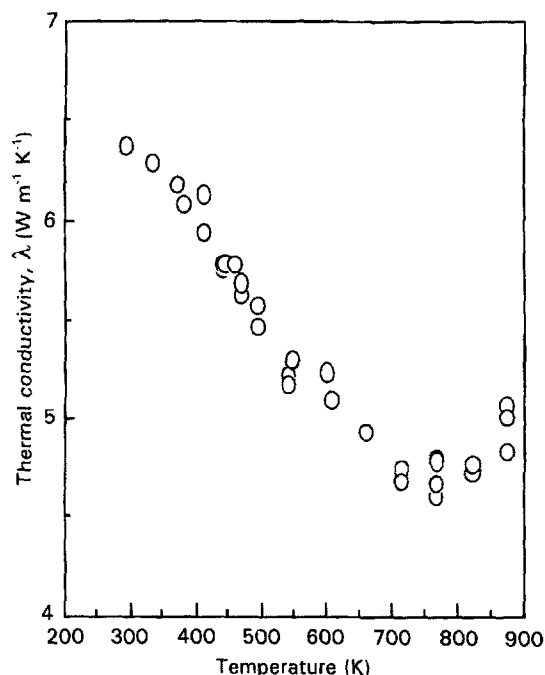


Figure 8 Temperature dependence of the thermal conductivity of Fe $_{0.92}$ Ru $_{0.05}$ Cr $_{0.03}$ Si $_2$. H.P. Cr 3% Ru 5%.

In these figures, the power factors of β -FeSi $_2$ -based materials, (Fe,Mn)Si $_2$ for p -type and (Fe, Co)Si $_2$ for n -type [2, 11], are also calculated and shown.

The power factors of all specimens exhibit broad maxima at around 800 K. The samples with optimum thermoelectric properties were obtained by high-pressure sintering for both p -type and n -type materials. The optimum composition for p -type material is found to be Fe $_{0.92}$ Ru $_{0.05}$ Cr $_{0.03}$ Si $_2$, and the power factor of this material is higher than that of p -type FeSi $_2$ in the whole temperature range. Fe $_{0.92}$ Ru $_{0.05}$ Co $_{0.03}$ Si $_2$ is a candidate as n -type material. The power factor of this material becomes higher than that of n -type-FeSi $_2$ above 800 K.

In order to estimate the figure of merit (Z) for thermoelectric conversion, thermal conductivity (λ) was measured by a conventional laser-pulse method for Fe $_{0.92}$ Ru $_{0.05}$ Cr $_{0.03}$ Si $_2$ sintered under high-pressure conditions. Fig. 8 shows the temperature dependence of the thermal conductivity of the specimen. The thermal conductivity exhibits its minimum value at around 800 K.

The figure of merit (Z) for thermoelectric conversion was calculated by Equation 1.

$$Z = \sigma \alpha^2 / \lambda \quad (1)$$

The Z -values of Fe $_{0.92}$ Ru $_{0.05}$ Cr $_{0.03}$ Si $_2$ are shown in Fig. 9 as a function of temperature. The Z -values of Fe $_{0.92}$ Ru $_{0.05}$ Cr $_{0.03}$ Si $_2$ are higher than that of p -type FeSi $_2$ [12] over the whole temperature range, indicating a possible application for a high temperature thermoelectric conversion system. The maximum value of Z is 3.5×10^{-4} (K $^{-1}$) at 750 K.

4. Conclusion

In summary, thermal stability and the thermoelectric properties of β -FeSi $_2$ are successfully improved by partial substitution of an Ru atom onto an Fe-site. High-pressure sintering is also effective in improving the figure of merit (Z) for thermoelectric conversion. Cr or Co-doped β -Fe $_{1-x}$ Ru $_x$ Si $_2$ solid solutions are candidate materials for thermoelectric modules for a high temperature thermoelectric energy conversion system.

Acknowledgements

The authors would like to thank Dr T. Sekino at Osaka University for helpful advice on the thermal conductivity measurements. This work has been supported by a Grant-in-Aid for Scientific Research on

Priority Areas: Energy Conversion and Utilization with High Efficiency, of the Ministry of Education, Science and Culture, Japan.

References

1. R. M. WARE and D. J. MCNEILL, *Proc. IEE* **111** (1964) 178.
2. I. NISHIDA, *Phys. Rev. B* **7** (1973) 2710.
3. C. LE. CORRE and J. M. GENIN, *Phys. Stat. Sol. (b)* **51** (1972) K85.
4. Y. DUSAUSOY, J. PROTAS, R. WANDJI and B. ROQUES, *Acta Crystallog. B* **27** (1971) 1209.
5. I. ENGSTRÖM, *Acta Chem. Scandinavica* **27** (1970) 2117.
6. K. MASON and G. MÜLLER-VOGT, *J. Cryst. Growth* **63** (1983) 34.
7. P. ECKERLIN and H. KANDLER, in Landolt Börnstein, "Numerical Data and Functional Relationships in Science and Technology, New Series", Vol. 6, p. 866, edited by K. H. Hellwege and A. M. Hellwege (Springer-Verlag, Berlin/Heidelberg/New York, 1971).
8. T. ENDO, Y. SATO, H. TAKIZAWA and M. SHIMADA, *J. Mater. Sci. Lett.* **11** (1992) 424.
9. J. K. BURDETT, *J. Solid. State. Chem.* **45** (1982) 399.
10. Y. OHTA and D. G. PETTIFOR, *J. Phys. Condens. Matter.* **2** (1990) 8189.
11. T. KOJIMA, *Phys. Stat. Sol. (a)* **111** (1989) 233.
12. I. NISHIDA, *Kogyo Zairyo* **33** (1985) 108. [in Japanese]

Received 18 May 1993

accepted 9 June 1994